

Spiral turbulence: from the oxidation of CO on Pt(110) to ventricular fibrillation*

ASHWIN PANDE,¹ SITABHRA SINHA^{1,2} AND RAHUL PANDIT^{1,2}

¹Department of Physics, Indian Institute of Science (IISc), Bangalore 560012, India

²Jawaharlal Nehru Centre for Advanced Scientific Research (JNCASR), Bangalore 560064, India.

Abstract

We give a brief overview of systems that show spiral patterns and spatiotemporally chaotic states. We concentrate on two physical systems: (1) the oxidation of CO on Pt(110) and (2) ventricular fibrillation in hearts. Simple models for these two different systems are closely related as they are both *excitable media*. We present these equations and give a short summary of the phenomena they yield.

1. Introduction

Spiral waves are found in a wide variety of physical, chemical and biological systems. These include convection patterns in cylindrical cells,¹ patterns in the Belousov-Zhabotinsky chemical reactions,^{1,2} the oscillations of cyclic-AMP in aggregating *Dictyostelium Discooidium* amoebae,^{1,3} the oxidation of carbon monoxide (CO) on surfaces of platinum single crystals,^{4,5} calcium waves in the cell cytoplasm⁶ of *Xenopus Laevis* oocytes, and in ventricular fibrillation⁷ which is perhaps the most dangerous form of cardiac arrhythmia. A variety of mathematical models have been used to describe these phenomena; we refer the reader to the review by Cross and Hohenberg for a recent discussion of many such models.¹ The models range from cellular automata⁸ to deterministic partial differential equations such as the complex Ginzburg-Landau equation (for oscillatory chemical reactions near onset) and equations in the FitzHugh-Nagumo class (for CO oxidation and ventricular fibrillation). We concentrate on the FitzHugh-Nagumo types of equations here. The description is not very technical since the talk on which this article is based was aimed at an audience drawn from different disciplines. We begin with a brief overview of phenomena followed by an introduction to equations in the FitzHugh-Nagumo class. We then present some results for specific models suggested for the oxidation of CO on Pt(110)^{4,5} and ventricular fibrillation⁹ including our recent studies.¹⁰

Many chemical reactions display spontaneous spatial self-organisation if the reactors are not stirred and the reactants are fed at a constant rate. Among these reactions, the oxidation of CO on Pt(110) has been studied in great detail.^{4,5} The experimental set-up consists of a cell containing a Pt wafer kept at a constant temperature. The reactants are fed into the cell at a constant rate and the products removed. Spatial structures in the concentration fields of the reactants have been observed by using photoelectron emission microscopy (PEEM). For a picture of the growth of a spiral wave on such a Pt(110) wafer, see Jakubith *et al.*⁴

*Text of lecture delivered at the Annual Faculty Meeting of the Jawaharlal Nehru Centre for Advanced Scientific Research at Bangalore on November 13, 1998.



FIG. 1. A spiral wave on a canine heart imaged using voltage-sensitive dyes and CCD cameras, after Witkowski *et al.*¹⁴ Image obtained from and reproduced with the permission of W. Ditto.

A human heart consists of four chambers—the two upper atria and two lower ventricles. Heart activity is driven by periodic signals emitted by the cells of the sinus node situated in the upper right atrium. These cells initiate the heartbeat cycle by emitting a pulse of electrical activity. This activity travels as a wave across the atria and stimulates the nerves of the atrioventricular node (AVN). From the AVN the signal travels along the His bundle and into the ventricles via the Purkinje fibre network which extensively innervates the ventricular wall. The ventricles now contract thus completing the beat cycle. Cardiac arrhythmia is caused when the signal from the sinus node does not propagate in the normal manner. Especially dangerous is ventricular fibrillation, an irregular pulsation of the ventricles, which is a major cause of death in the industrialised world.¹¹ It has been conjectured for many years¹² that ventricular fibrillation is associated with the formation of spiral waves (or their three-dimensional analogues called scroll waves) on the walls of the ventricles. Experimental evidence for such spiral waves has been increasing with the advent of voltage-sensitive dyes and advanced imaging techniques.^{13, 14} Figure 1 shows such a spiral wave on the ventricle of a canine heart. Such spirals have also been seen to break up.

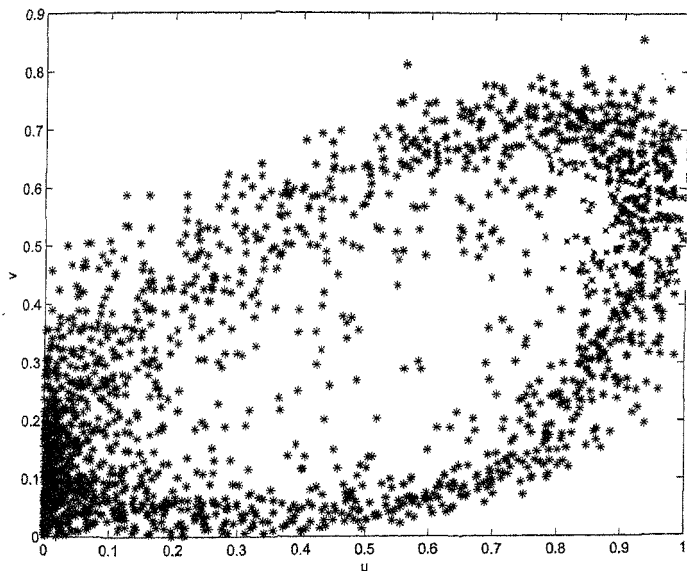


FIG. 2. The local phase portrait in the state T1 of model 2 at $\varepsilon = 0.0781$. Such local phase portraits get progressively more disordered in the regimes M, T1 and T2.

Both the oxidation of CO on Pt (110) and ventricular fibrillation have been the focus of many theoretical studies. These are motivated partially by a desire to understand the phenomena seen in experiments and partially to elucidate the general properties of systems displaying such spatiotemporally chaotic, statistical steady states. The remainder of this paper is organised as follows: Section 2 consists of an introduction to FitzHugh–Nagumo equations and the models we consider. Section 3 describes some results for the model of CO oxidation on Pt(110). Section 4 describes some results for the model of ventricular fibrillation. Section 5 ends with concluding remarks.

2. Models

FitzHugh–Nagumo-type equations belong to the general class of reaction–diffusion equations. These are of the form

$$\frac{\partial U_i}{\partial t} = f_i(U_j) + D_{ij} \nabla^2 U_j, \quad (1)$$

where the f_i are nonlinear functions of the U_j s and D_{ij} are elements of a matrix of diffusion constants. The FitzHugh–Nagumo-type system used by Hildebrand *et al.*⁵ for the oxidation of CO on Pt(110) is

$$\begin{aligned}\frac{\partial u}{\partial t} &= \nabla^2 u - \frac{1}{\varepsilon} u(u-1)(u-(v+b)/a), \\ \frac{\partial v}{\partial t} &= f(u) - v;\end{aligned}\quad (2)$$

here the fields u and v are related to the CO coverage and the surface reconstruction, a , b , and ε are control parameters. Physically ε is proportional to the ratio of the rate constant for the change in surface structure to the rate constant for the oxidation of adsorbed CO on the surface. Further, $f(u) = 0$ if $u < \frac{1}{3}$, $f(u) = 1 - 6.75u(u-1)^2$ if $\frac{1}{3} \leq u < 1$, and $f(u) = 1$ if $u \geq 1$. The form of $f(u)$ leads to the production of v only above a certain threshold value of u . This is an effective model with u and v related to reactant coverages and surface reconstruction. We refer the reader to Jakubith *et al.*⁴ and Hildebrand *et al.*⁵ for further details and the specific form for $f(u)$ which has been found to model CO oxidation on Pt(110) experiments well. We have studied model 2 with both periodic and Neumann (no-flux) boundary conditions. Here we restrict ourselves to Neumann boundary conditions for ease of comparison with model 3.

The Panfilov–Hogeweg model for ventricular fibrillation that we consider is⁷

$$\begin{aligned}\frac{\partial e}{\partial t} &= \nabla^2 e - f(e) - g, \\ \frac{\partial g}{\partial t} &= \varepsilon(e, g)(ke - g),\end{aligned}\quad (3)$$

where e is the transmembrane potential and g a recovery variable corresponding to the amount of openness of the ion channels.¹² Also, $f(e) = C_1 e$ if $e < e_1$; $f(e) = -C_2 e + a$ if $e_1 \leq e \leq e_2$; $f(e) = C_3(e - 1)$ when $e > e_2$, and $\varepsilon(e, g) = \varepsilon_1$ when $e < e_2$; $\varepsilon(e, g) = \varepsilon_2$ when $e > e_2$, and $\varepsilon(e, g) = \varepsilon_3$ when $e < e_1$ and $g < g_1$. Physically $\varepsilon(e, g)$ ⁻¹ determines the refractory time period of this model of ventricular muscle. Since the ventricles are electrically insulated from the atria, we impose Neumann boundary conditions.

3. CO Oxidation on Pt(110)

For the model of CO oxidation on Pt(110) (2), Hildebrand *et al.*⁵ find that there are many different statistical steady states. These include states with no waves (N), with flat-shrinking waves (F), with rigidly rotating spirals (S), with meandering spirals (M) and turbulent states with creation and annihilation of spirals (T1 and T2). These authors have found a stability or 'phase' diagram in the $b - \varepsilon$ plane for $a = 0.84$, and have calculated the spatial autocorrelation function of the density of spiral cores $\langle n(\vec{x}, t)n(\vec{x} + \vec{s}, t) \rangle$. They suggest that the change in the spiral dynamics on passing from T1 to T2 is like a 'liquid-gas' transition. We have simulated model 2 by discretising it on a square lattice and using a variable stepsize fourth-fifth order Runge–Kutta integrator for time stepping.¹⁵ In some cases, we also use a fast inte-



FIG. 3. A plot of $u(\bar{x})$ as a function of space in model 2. The colour at a point is proportional to the value of u at that point, obtained after evolving a typical initial condition for 5000 time units. Note the similarity of this figure with Fig. 5. For this figure, $\varepsilon = 0.073$ corresponds to T1 state.

gration scheme proposed by Barkley¹⁶ and developed by Doule *et al.*¹⁷ We have used Neumann boundary conditions to compare with model 3. We have investigated the local dynamics, i.e. the dynamics obtained by plotting $u(\bar{x}_n, t_n)$ vs $v(\bar{x}_n, t_n)$, $n = 1, 2, \dots$ for fixed spatial location \bar{x}_n and $t_n = n\Delta$ where Δ is a sampling interval which we choose to be $= 0.1$ time units. Such local phase portraits show that, in the states S, M, and T1, the system displays oscillatory behaviour; a representative phase portrait is shown in Fig. 2 for T1.

The trajectory in the local phase portrait loops around the fixed point $(u_*, v_*) \simeq (0.66, 0.484)$ of eqn (2) without the ∇^2 term. We define the phase $\phi(\mathbf{x}, t) \equiv \tan^{-1}((v(\mathbf{x}, t) - v_*) / (u(\mathbf{x}, t) - u_*))$ and note that it winds by 2π around the cores of spiral defects. Thus, it can be used to obtain the defect density ρ .¹⁰ (Fig. 4)

4. Ventricular fibrillation

It is believed that ventricular fibrillation occurs because of the spontaneous breakdown of contraction waves in the heart muscle leading to a state with many rotating spirals.¹²⁻¹⁴

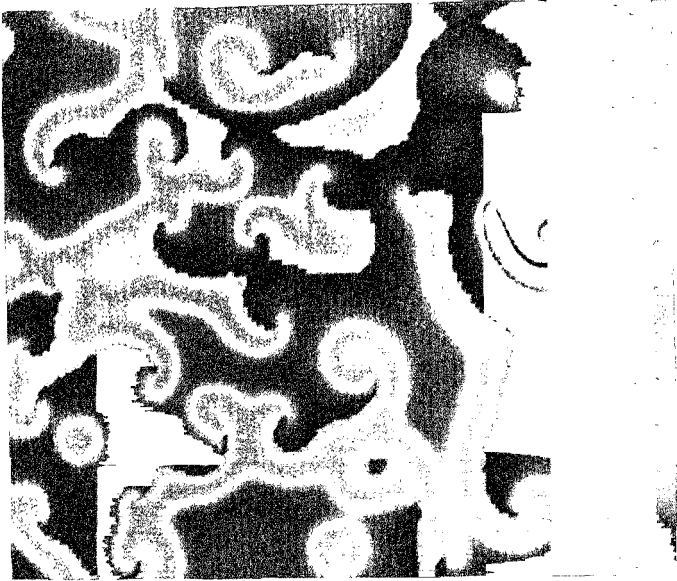


FIG. 4. Phase ϕ (see text) corresponding to the field configuration of Fig. 3 as a function of space. The colour at a point is proportional to the value of the phase at that point.

Physiological abnormalities do not seem to play an important role in this arrhythmia in a sizeable fraction of cases. Thus, it is interesting to study models in which spiral break up appears spontaneously without introducing spatial inhomogeneities in the diffusion constant, for example. For model 3, Panfilov⁹ finds that, for parameter values $e_1 = 0.0026$, $e_2 = 0.837$, $C_1 \approx 20$, $C_2 = 3$, $C_3 = 15$, $a = 0.06$, $k = 3$, $\epsilon_1^{-1} = 75$, $\epsilon_2^{-1} = 1$, $g_1 = 1.8$ and $0.5 < \epsilon_3^{-1} < 10$, an initial condition in the shape of a broken wave gives rise to states containing many spirals. They have also calculated an electrocardiogram (ECG) numerically for this model in the turbulent state. In this section, we elucidate the spatiotemporal nature of the chaotic behaviour of this system. Panfilov⁹ notes that the breakdown of spirals in models 2 and 3 is qualitatively similar. We elaborate on this similarity below. The state with broken spirals in model 3 is similar to the state T1 in model 2 as can be seen by comparing Figs 5 and 3.

We have simulated model 3 using finite-differencing in space with a forward-Euler algorithm for time stepping. Most of our simulations are done with a system size of 256×256 with a spatial grid step of $dx = 0.5$ and a time step of $dt = 0.022$. Physically one time unit is equal to 5 milliseconds and one spatial unit is equal to 1 millimeter. We use the parameter



FIG. 5. The configuration of the e field of model 3 on a system of size 256×256 obtained after evolving a typical initial condition for 1,000 time units.

values given above. We have calculated a local phase portrait for this model, i.e. a plot of $e(\tilde{x}_n, t_n)$ vs $g(\tilde{x}_n, t_n)$ for a fixed spatial location \tilde{x}_n (Fig. 6). Note that this local phase portrait is similar to that of T1 state of CO oxidation (model 2).

We find that for a system of size 50×50 the lifetime τ_t of the turbulent state is ≈ 300 time units. After this time, the entire field configuration goes to zero for various initial conditions. For a system of size 100×100 $\tau_t \approx 950$ time units. We conjecture that τ_t grows with system size; we are investigating this scaling of τ_t . The typical size of a human heart corresponds to a system size of $\approx 600 \times 600$ so the size dependence of τ_t is of obvious interest. We note in passing that this qualitative trend of τ_t increasing with system size is in accord with the well-known phenomenon that only the larger mammals have heart attacks.

To characterise chaos in model 3, we have calculated the maximum Lyapunov exponent λ_{\max} for a system of size 128×128 . The maximum Lyapunov exponent measures the divergence of nearby trajectories in the system. To calculate it we use standard methods.¹⁸ In the transient turbulent state of model 3, λ_{\max} saturates to a value of ≈ 0.2 . (Fig 7).

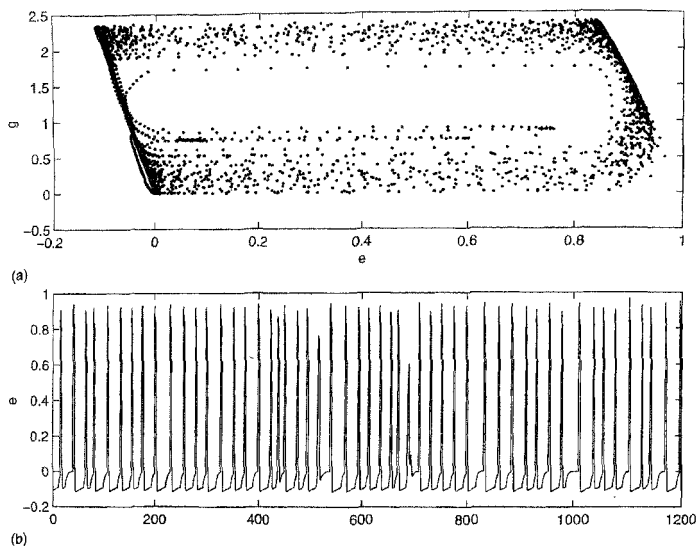


FIG. 6(a). A local phase portrait of model 3; (b) a time series of the transmembrane potential ϕ . The system size was 256×256 with a grid spacing of 0.5.

Note that when this transient decays, the maximum Lyapunov exponent decreases to negative values.

5. Conclusions

Spiral patterns are seen in a wide variety of natural systems.¹ Here we have concentrated on two such systems which are also excitable media. The chaotic states of these systems display the break up of large spirals into smaller ones in the states T1 and T2. The qualitative similarity of such spiral break up in models 2 and 3 has been mentioned briefly earlier.⁹ Here we have elucidated this similarity by comparing the spiral patterns (Figs 2 and 6) in state T1 of model 2 and the chaotic state of model 2; local phase portraits (Figs 2 and 6) are also similar. We have characterized the chaos in model 3 by computing the maximum Lyapunov exponent λ_{\max} (Fig. 7) as we have done for model 2 elsewhere.¹⁹

Our study shows considerable similarity between the behaviour of model 2 in state T1 and model 3 for the parameter values given above. It should be possible to exploit this similarity to gain new insights into these two excitable media (e.g. by conducting experiments on the oxidation of CO on Pt(110) which might be hard to do on a human heart). Of

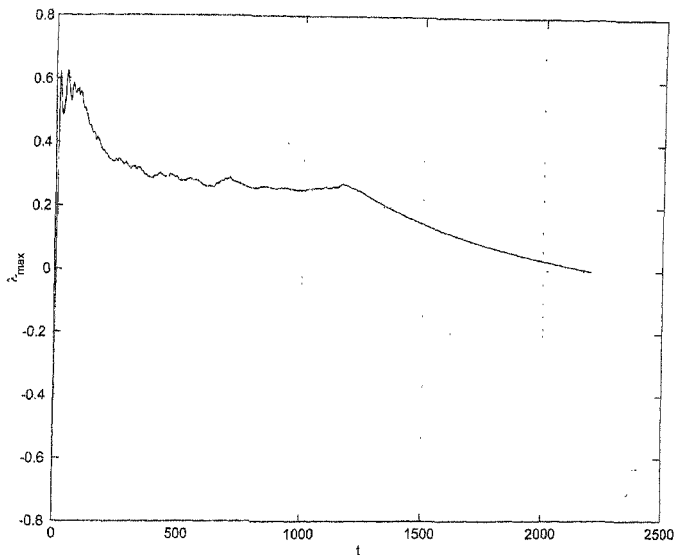


FIG. 7. The approximation to the maximum Lyapunov exponent λ_{\max} at times t vs t . Note that λ_{\max} approaches a positive constant (≈ 0.2) and then decays at large times to negative values. This occurs because there is a long-lived chaotic transient which finally decays to a state that is constant in space with $e(\vec{x}, t) = 0$ and $g(\vec{x}, t) = 0$ everywhere. The lifetime of this chaotic transient increases with the size of the system (see text).

course, some caution must be exercised while doing this for the two models are different in some respects: the chaotic state of model 3 is a transient for the system sizes we have studied, whereas the analogous state for model 2 seems to be a statistical steady state; furthermore, if the ∇^2 terms are dropped in both the models, then model 2 has an extra unstable fixed point [at $(u, v) = (u_*, v_*)$], i.e. the reaction kinetics are different in the two models. We hope that our work will stimulate experimental studies that will try to elucidate the similarities and differences between spiral turbulence in the oxidation of CO on Pt(110) and ventricular fibrillation. Since ventricular fibrillation in cardiac muscle is fatal,^{7, 11, 12} any insight gained into it by studying similar systems is of great interest.

Acknowledgement

We thank the Council of Scientific and Industrial Research (CSIR) and JNCASR for support and Supercomputer Education Research Centre (SERC), IISc, for computational facilities and W. Ditto for permission to reproduce Fig. 1 from his home page.

References

1. CROSS, M. C. AND HOHENBERG, P. C. *Rev. Mod. Phys.*, 1993, **65**, 851–1111.
2. WINFREE, A. T. *Science*, 1972, **175**, 634–636.
3. SIEBERT, F. AND WEIJER, C. J. *Physica D*, 1991, **49**, 224–232.
4. JAKUBITH, S. *et al.* *Phys. Rev. Lett.*, 1990, **65**, 3013–3016.
5. HILDEBRAND, M., BAR, M. AND EISWIRTH, M. *Phys. Rev. Lett.*, 1995, **75**, 1503–1506.
6. LECHLEITER, J. D. *et al.* *Science*, 1993, **252**, 123–126.
7. GLASS, L. *Phys. Today* (Pt. 1), 1996, **49**, 40–45.
8. GERHARDT, M. *et al.* *Science*, 1990, **247**, 1563–1566.
9. PANFILOV, A. V. *Chaos*, 1998, **8**, 57–64.
10. PANDE, A. AND PANDIT, R. *Structure and dynamics of materials in the mesoscopic domain* (B. D. Kulkarni and Moti Lal, eds), Imperial College Press–The Royal Society (in press).
11. WINFREE, A. T. *Chaos*, 1998, **8**, 1–19.
12. WINFREE, A. T. *When time breaks down*, Princeton University Press, 1987.
13. WITKOWSKI, F. X. *et al.* *Nature*, 1998, **392**, 78–82.
14. GRAY, R. A. *et al.* *Nature*, 1998, **392**, 75–78.
15. PRESS, W. H. *et al.* *Numerical Recipes in C*, Cambridge University Press, 1995.
16. BARKLEY, D. *Physica D*, 1991, **49**, 61–70.
17. DOULE, M. *et al.* *Int. J. Bifurcation Chaos*, 1997, **7**, 2529–2545.
18. PARKER, T. AND CHUA, L. *Practical numerical algorithms for chaotic systems*, Springer, 1989.
19. PANDE, A. AND PANDIT, R. to be published.